

Removal of Amitraz with Synthesized Nano TiO₂ Rods

Razieh Razavi^{*1}, Moslem Basij², Marzieh Salajgheh¹

¹ Department of Chemistry, Faculty of Science, University of Jiroft, Jiroft, Iran

² Department of Plant Protection, Faculty of Agriculture, University of Jiroft, Jiroft, Iran

Received: 7 June 2024

Accepted: 4 September 2024

DOI: [10.30473/IJAC.2025.72870.1310](https://doi.org/10.30473/IJAC.2025.72870.1310)

Abstract

Amitraz removal was investigated by synthesized TiO₂ from an aqueous solution. For this propose, FT-IR, XRD, UV-Vis, SEM and EDS were used to characterize the synthesized nano adsorbents and to determine the removal process. Batch adsorption studies were conducted to investigate the effect of temperature, initial Amitraz concentration, adsorbent count and contact time as important adsorption parameters. The maximum equilibrium time was found to be 15 min with 5 mg adsorbent in 35°C at pH=7 for TiO₂. All the adsorption equilibrium data were well fitted to the Freundlich isotherm model with heterogenous, multilayer, temperature depended, irreversible and spontaneously behavior. The ΔH is -4.2×10^3 kJ and ΔS is $15 \text{ J mol}^{-1} \text{ K}^{-1}$.

Keywords

Amitraz; Removal; TiO₂; Adsorbent; Isotherm; Kinetics.

1. INTRODUCTION

Amitraz[1–4] is a widely used and effective insecticide and acaricide, mainly used in veterinary medicine to control ticks, mites and lice on animals (Farmer and Seawright and in agriculture to control fruit tree and cotton pests. In some countries it has been also registered for the use in apiculture to control the varroa mite (Varroa destructor). Its effectiveness and wide spectrum can be explained by its several biochemical targets, including the inhibition of monoamine oxidases and the activation of octopamine receptors [5-6]. Once in the environment, due to its high log Kow (5.34–5.5), amitraz is expected to adsorb to soil and sediment and to quickly metabolize into persistent and more water-soluble products [7]. However, in several countries, due to its widespread use and high direct application rate, there is an elevated risk of run-off and contamination of adjacent aquatic ecosystems. Since parent amitraz is short-lived in the environment, it is not expected to pose a major concern for aquatic invertebrates, as opposed to some more stable and toxicologically relevant metabolites that retain toxic activity [5].

The release of neonicotinoid pesticides [8–12] is a significant concern for the environment due to their high mobility in the soil and the contamination of groundwater and surface water. For example, imidacloprid is one of the most widely used neonicotinoid pesticides, effective against agricultural pests, so it appears in the aquatic environment in increasing concentrations, affecting insects, birds, crustaceans, fish, and

organisms in the soil by increasing acidity. Advanced oxidation processes (AOP) are degradation processes of organic pollutants, in particular pesticides, based on reactive oxygen species (ROS) generated on the photocatalyst surface [13-14, 23–25, 15–22]. Titanium oxide-based heterogeneous photocatalysis [26-27, 36–42, 28–35] for pollutant degradation has been investigated over decades and is based on the reaction between a broad range of organic pollutants and ROS species [17]. In this scientific work, adsorption of Amitraz on TiO₂ considered. The parameters which affected on adsorption were studied and isotherms were investigated.

2. EXPERIMENTAL

Amitraz, Sulfuric acid, Hydrochloric acid and Ethanol were purchased from Merck Company.

2.1. Synthesis of TiO₂

For synthesis of TiO₂, leaching process was applied [43] That is, The ilmenite concentrate was received from Kahnooj/Iran processing plant (Iran) mine. Leaching experiments were carried out under sulfuric acid leaching process. 0.5g TiFeO₃ was added to 20mL pure H₂SO₄(Merck,Germany) by 120°C heat. After 30 min the mixture was filtered, and then H₂O was added to precipitate in ultra-sounding bath at 50°C for 15 min. Leaching experiments were carried out under Hydrochloric acid leaching process. 1g of thermal treatment TiFeO₃ was added to 100 mL HCl 6M (Merck,Germany) with 100°C heat. After 8 hours the mixture was filtered, and then HCl was added

* Corresponding author:

to wash the precipitate. This process repeated for three times to attain pure rutile. The precipitate has calcinated for 1 hour at 950°C. Before using an ilmenite concentrate (Kahnootj/ Iran), the ilmenite concentrate was given a thermal pre-leach treatment (oxidation at 800°C, for 30 min and reduction in argon at 950°C, for 1h and 1/0.75 ratio of ilmenite to active coal and finally cooling in nitrogen. The pre-leach thermal treatment converts most of the contained iron back to the ferrous state, and transforms the pseudorutile phase.

2.2. TiO_2 characterization

The phase and crystal structure of the samples were analyzed via X-ray diffraction technique (X'Pert Pro, Netherland, Panalytical Company) with $Cu-K\alpha$ as basis of energy. The TESCAN MIRA3 field emission scanning electron microscope (FE-SEM) (Czech Republic) integrated with EDS detector was utilized for imaging and elemental analysis of prepared nanostructures. Infrared (IR) spectra was obtained with a SHIMADZU spectrophotometer, over a scan range of 500 cm^{-1} - 4000 cm^{-1} .

2.3. Adsorption experiments

The present research carried out Amitraz equilibrium adsorption on TiO_2 . The study also considered constant concentrations of amitraz in different time and temperature conditions with the use of an orbital shaker which operated at 150 rpm agitation speed. It also utilized 5 ppm stock solutions of Amitraz. Analysis of the solution for concentrations of Amitraz and its adsorption on the adsorbent at equilibrium time with the use of UV-Visible spectroscopy were conducted following magnetic separation and filtration. The relation below was used to calculate the amitraz adsorption on the adsorbent at equilibrium time of q_e :

$$q_e = \frac{V \times (C_0 - C_e)}{m} \quad (1)$$

In which, C_0 , C_e , V , and m represent the primary Amitraz concentrations (mg/L), Amitraz concentrations (mg/L) in solution following the adsorption, the solution volume (L), and the mass (g) of TiO_2 . the following relation was used to calculate the percentage of Amitraz removal:

$$(\% R) = \frac{C_0 - C_t}{C_0} \times 100 \quad (2)$$

In which, C_0 and C_t indicate the primary Amitraz solution concentrations (mg/L) and the ultimate concentrations (mg/L) following the process of adsorption, respectively. Relation 3 was used to calculate adsorption capacity from the adsorbent mass and Amitraz solution volume:

$$q_{t(mg)} = \frac{V \times (C_0 - C_t)}{m} \quad (3)$$

In which m and V represent the adsorbent dose (mg) and Amitraz solution volume (L).

3. RESULTS AND DISCUSSION

3.1. Characterization of TiO_2

The X-ray diffraction patterns of TiO_2 in Fig. 1. Shown that the main peak on 2θ 27.5° , 36° , 41.5° , 54.2° , 56.5° , 63° and 65° refers to TiO_2 in rutile forms. Some extra peaks were appeared in XRD pattern which can refer to non-pure forms of TiO_2 . The position of 2θ at 27.42° , 36.08° , 41.25° , 54.33° and 63.44° corresponds to Miller indices of (110), (101), (111), (211) and (002) plane, respectively [44].

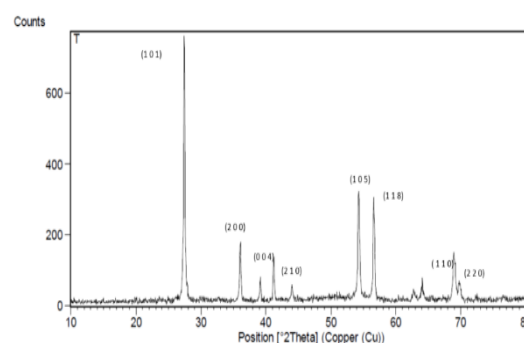


Fig. 1. The XRD pattern of TiO_2 .

Infrared spectrum of the synthesized TiO_2 nanoparticles was in the range of 500 - 4000 cm^{-1} wave number which identifies the chemical bonds as well as functional group in the compound (Fig. 2). The broad intense band below 1200 cm^{-1} is due to $Ti-O-Ti$ vibrations [45].

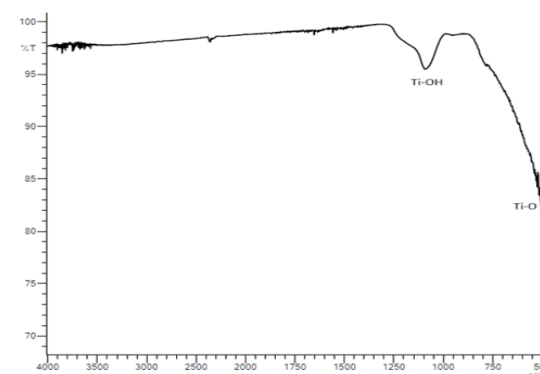


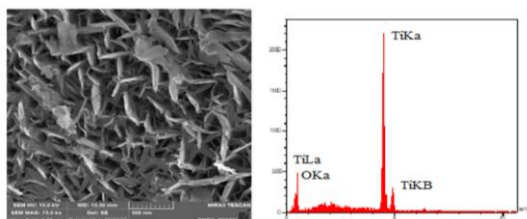
Fig. 2. The IR spectrum of TiO_2

3.2. Morphology of TiO_2

The synthesized TiO_2 's topographical features were investigated using a scanning electron microscope. As depicted in Fig. 3, the nanoparticles of TiO_2 showcased a rod-like configuration, with widths ranging 97nm.

Table 1. % weight of each atom in TiO₂ (EDX)

Elt	Line	Int	Error	K	Kr	W%	A%
O	Ka	66.1	15.1934	0.1073	0.0638	41.31	67.82
Ti	Ka	614.9	1.3418	0.8927	0.5309	58.69	32.18
				1.0000	0.5947	100.00	100.00

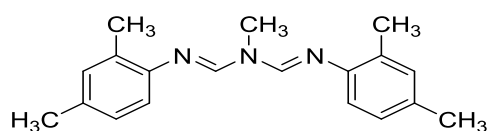
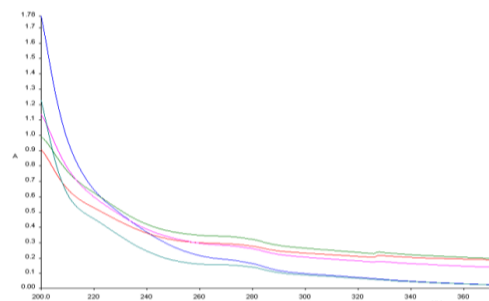
**Fig. 3.** SEM and EDX TiO₂.

Energy dispersive spectrometry (EDX), an X-ray analytical technique, facilitates the swift acquisition of elemental concentrations Table 1. These concentrations can be procured from specific points, traced along lines, or mapped. A two-dimensional representation of the distribution of elements within the sample can be produced by displaying the characteristic X-ray intensities or elemental concentrations. Fig. 4 demonstrates a uniform distribution of the O and Ti elements within the nanorods.

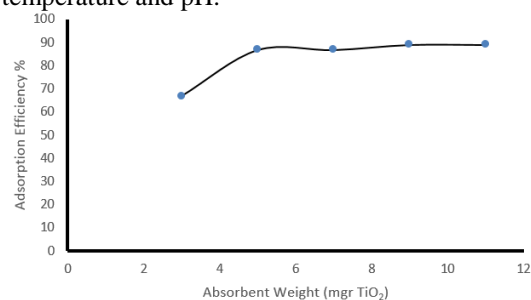
**Fig. 4.** Map of TiO₂.

3.3. Adsorption analysis

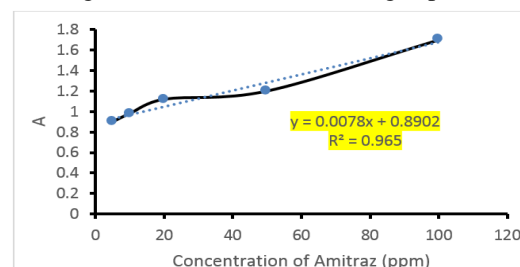
Fig. 5 indicates the UV-Vis spectrum of Amitraz. UV-Vis spectrum indicated the transition electrons between occupied or unoccupied electron layers. Electrons on n , σ and π levels have sharp peaks on the UV-Vis spectrum. n electrons are nonbinding electrons that appeared around O, N, S and Halogen atoms. These electrons need low energy ($n \rightarrow \pi^*$) and in 150-250 nm, which is not presented in the UV-Vis spectrum. Transitions of ($n \rightarrow \pi^*$) and ($\pi \rightarrow \pi^*$) appeared at 200-700 nm and are very important. These transitions referred to unsaturated and aromatic molecules which are chromophores. According to the Fig. 5. peak at 260-280 nm, it can result that Amitraz has n atoms and ($n \rightarrow \pi^*$) transitions and this peak applied for analyzing the adsorption process. In Schematic 1 the structure of Amitraz demonstrate.

**Schem. 1.** Structure of Amitraz**Fig. 5.** UV-Vis spectrum of Amitraz in different concentration.

In this study, the TiO₂ was used to remove the Amitraz from water. For this purpose different masses of nano TiO₂ powder was applied for removing the different concentrations of Amitraz in the solution in various conditions such as time, temperature and pH.

**Fig. 6.** Effect of adsorbent (TiO₂) on adsorption efficiency.

As shown in Fig. 7. the weight of TiO₂ which applied is 3,5,7,9 and 11 mg and according to the data plotted 5 mg of TiO₂ is the weight that can optimized for applying adsorption. It can be observed that by rising the weigh the adsorption efficiency is constant. Therefore, it is clear that the last weight must be selected for doing experiments.

**Fig. 7.** Calibration curve of Amitraz concentration For detection the concentration of adsorbed Amitraz, knowing the adsorb of it on different concentration is necessary therefore the calibration curve of Amitraz illustrated in Fig. 7. According

to Fig. 7. it is understood that the linear adsorption area for Amitraz is under 5 ppm. Therefore, for optimizing the Amitraz concentration (Fig. 8), the 1, 3, 5, 7, 10 ppm of Amitraz with 5 mg of TiO₂ examined. The Results showed that concentration 5 ppm of Amitraz has best result for adsorb process.

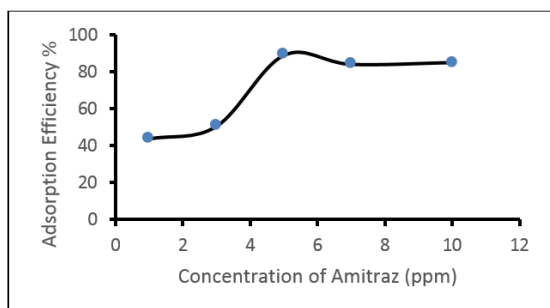


Fig. 8. Optimizing of Amitraz concentration.

In the structure of Amitraz, three nitrogen atoms appeared therefore, Amitraz has three non-bond electron that can give H⁺ ion. Consideration effect of pH on adsorption process demonstrated that adsorption efficiency decreased when pH increased Fig. 9.

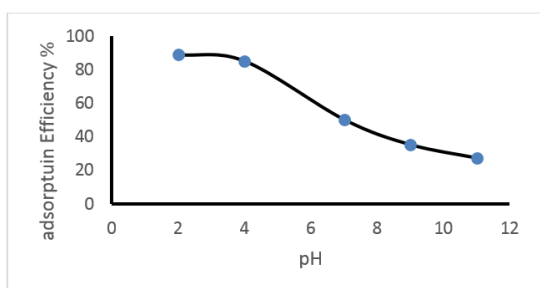


Fig. 9. Effect of pH on adsorption efficiency of Amitraz.

For detecting the effect of time on adsorption efficiency, in Fig. 10 the plot of time effect can be seen that resulted after 15 min the site of TiO₂ saturated. Increasing the temperature caused decreasing the adsorption efficiency of Amitraz. It resulted in kinetic energy of Amitraz molecules on TiO₂ surface get increased and move far from the TiO₂ surface Fig. 11.

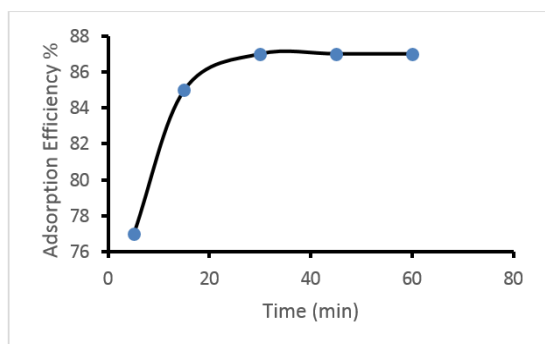


Fig. 10. Effect of time on Amitraz adsorption

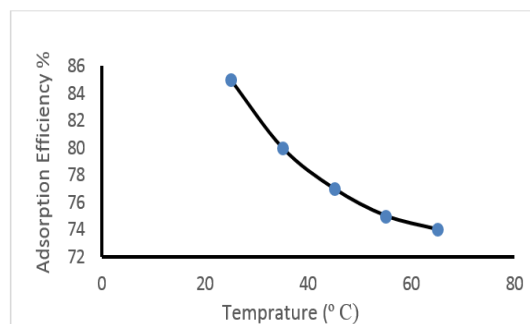


Fig. 11. Effect of temperature on Amitraz adsorption

Adsorption behaviour of Amitraz on TiO₂ can consider with isotherms. Further more Freundlich and Langmuir isotherms were plotted. Fig. 12 demonstrated the behaviour of adsorption. As shown in the Fig. 12 adsorption behaviour adapted with Frenudlich isotherm $R^2=0.97$. Therefore it can be resulted that adsorption of Amitraz is multilayer and irreversible and distribution of Amitraz is heterogenous on the surface of TiO₂ depended on temperature.

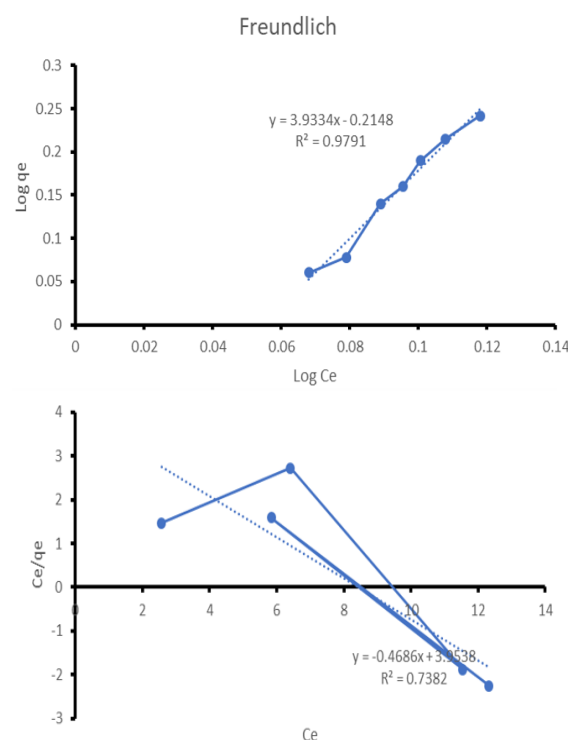


Fig. 12. Isotherms of adsorption Amitraz on TiO₂

Thermodynamic manner of amitraz adsorption is also important. Therefore in Fig 13 Log K plotted versus $1/T$ $R^2=0.97$ and the data shown that ΔH is -4.2×10^3 kJ and ΔS is $15 \text{ J mol}^{-1}\text{K}^{-1}$. These data means that the adsorption of Amitraz on TiO₂ is spontaneously.

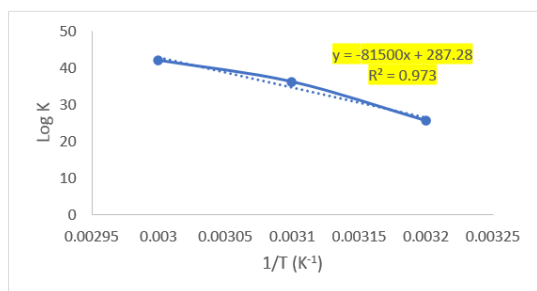


Fig. 13. Thermodynamic manner of Amitraz adsorption on TiO₂.

4. CONCLUSIONS

In the present research Adsorption of Amitraz on TiO₂ was investigated. Some parameters such as concentration of Amitraz, time, temperature, adsorbent amount and pH were considered. The data showed adsorption of Amitraz depended on time, temperature and pH. The results illustrated that this process is heterogenous, temperature depended, irreversible and spontaneously.

REFERENCES

- [1] E. Korta, A. Bakkali, L.A. Berrueta, B. Gallo, F. Vicente, S. Bogdanov, Determination of amitraz and other acaricide residues in beeswax, *Anal. Chim. Acta.* 475 (2003) 97–103.
- [2] A.C. Carranza-Martin, M.C. Fabra, N. Urrutia Luna, N. Farnetano, J.P. Anchordoquy, J.M. Anchordoquy, S.J. Picco, C.C. Furnus, N. Nikoloff, In vitro adverse effects of amitraz on semen quality: Consequences in bovine embryo development, *Theriogenology.* 199 (2023) 106.
- [3] S.T. O’Neal, C.C. Brewster, J.R. Bloomquist, T.D. Anderson, Amitraz and its metabolite modulate honey bee cardiac function and tolerance to viral infection, *J. Invertebr. Pathol.* 149 (2017) 119–126.
- [4] W.G. Maciel, W.D.Z. Lopes, B.C. Cruz, L.V.C. Gomes, W.F.P. Teixeira, C. Buzzulini, M.A. Bichuette, G.P. Campos, G. Felippelli, V.E. Soares, G.P. de Oliveira, A.J. da Costa, Ten years later: Evaluation of the effectiveness of 12.5% amitraz against a field population of *Rhipicephalus (Boophilus) microplus* using field studies, artificial infestation (Stall tests) and adult immersion tests, *Vet. Parasitol.* 214 (2015) 233–241.
- [5] H.R. Monteiro, M.F.L. Lemos, S.C. Novais, A.M.V.M. Soares, J.L.T. Pestana, Amitraz toxicity to the midge *Chironomus riparius*: Life-history and biochemical responses, *Chemosphere.* 221 (2019) 324–332.
- [6] N.N. Jonsson, R.J. Miller, D.H. Kemp, A. Knowles, A.E. Ardila, R.G. Verrall, J.T. Rothwell, Rotation of treatments between spinosad and amitraz for the control of *Rhipicephalus (Boophilus) microplus* populations with amitraz resistance, *Vet. Parasitol.* 169 (2010) 157–164.
- [7] Gao, Y. Tan, H. Guo, Simultaneous determination of amitraz, chlordimeform, formetanate and their main metabolites in human urine by high performance liquid chromatography–tandem mass spectrometry, *J. Chromatogr. B Anal. Technol. Biomed. Life Sci.* 1052 (2017) 27–33.
- [8] M.V.B. Zanoni, K. Irikura, J.A.L. Perini, G.G. Bessegato, M.A. Sandoval, R. Salazar, Recent achievements in photoelectrocatalytic degradation of pesticides, *Curr. Opin. Electrochem.* 35 (2022) 101020-101028.
- [9] H. Chawla, S. Garg, J. Rohilla, Á. Szamosvölgyi, A. Efremova, I. Szent, P.P. Ingole, A. Sápi, Z. Kónya, A. Chandra, Visible LED-light driven photocatalytic degradation of organochlorine pesticides (2,4-D & 2,4-DP) by *Curcuma longa* mediated bismuth vanadate, *J. Clean. Prod.* 367 (2022) 132923-132930.
- [10] M. Tang, Y. Ao, C. Wang, P. Wang, Facile synthesis of dual Z-scheme gC₃N₄/Ag₃PO₄/AgI composite photocatalysts with enhanced performance for the degradation of a typical neonicotinoid pesticide, *Appl. Catal. B Environ.* 268 (2020) 118395-118405.
- [11] A. Luna, R. Alonso, V.M. Cutillas, C.M. Ferrer, M.J. Gómez-Ramos, D. Hernando, A. Valverde, J.M. Flores, A.R. Fernández-Alba, A.R. Fernández-Alba, Removal of pesticide residues from beeswax using a methanol extraction-based procedure: A pilot-scale study, *Environ. Technol. Innov.* 23 (2021) 101606-101616.
- [12] T. Ahamad, S.M. Alshehri, Fabrication of Ag@SrTiO₃/G-C₃N₄ Heterojunctions for H₂ Production and the Degradation of Pesticides Under Visible Light, *SSRN Electron. J.* (2022) 4034212-403420.
- [13] N.T. Hanh, N. Le Minh Tri, D. Van Thuan, M.H. Thanh Tung, T.D. Pham, T.D. Minh, H.T. Trang, M.T. Binh, M.V. Nguyen, Monocrotophos pesticide effectively removed by novel visible light driven Cu doped ZnO photocatalyst, *J. Photochem. Photobiol. A Chem.* 382 (2019) 111923-111930.
- [14] L. Liu, X.L. Chen, M. Cai, R.K. Yan, H.L. Cui, H. Yang, J.J. Wang, Zn-MOFs composites loaded with silver nanoparticles are used for fluorescence sensing pesticides, Trp, EDA and photocatalytic degradation of organic dyes, *Spectrochim. Acta - Part A Mol. Biomol. Spectrosc.* 289 (2023) 122228-122238.

- [15] A. Sudhaik, P. Raizada, S. Thakur, R. V. Saini, A.K. Saini, P. Singh, V. Kumar Thakur, V.H. Nguyen, A.A.P. Khan, A.M. Asiri, Synergistic photocatalytic mitigation of imidacloprid pesticide and antibacterial activity using carbon nanotube decorated phosphorus doped graphitic carbon nitride photocatalyst, *J. Taiwan Inst. Chem. Eng.* 113 (2020) 142–154.
- [16] K. Bano, S. Kaushal, P.P. Singh, A review on photocatalytic degradation of hazardous pesticides using heterojunctions, *Polyhedron*. 209 (2021) 115465-115473.
- [17] L. ANDRONIC, M. LELIS, A. ENESCA, S. KARAZHANOV, Photocatalytic Activity of Defective Black-Titanium Oxide Photocatalysts Towards Pesticide Degradation Under Uv/Vis Irradiation, *SSRN Electron. J.* (2022) 4050210-4050221.
- [18] H. Adabavazeh, A. Saljooqi, T. Shamspur, A. Mostafavi, Synthesis of polyaniline decorated with ZnO and CoMoO₄ nanoparticles for enhanced photocatalytic degradation of imidacloprid pesticide under visible light, *Polyhedron*. 198 (2021) 115058-115068.
- [19] S.Y. Tan, W.C. Chong, S. Sethupathi, Y.L. Pang, L.C. Sim, E. Mahmoudi, Optimisation of aqueous phase low density polyethylene degradation by graphene oxide-zinc oxide photocatalysts, *Chem. Eng. Res. Des.* 190 (2023) 550–565.
- [20] M. Zangiabadi, A. Saljooqi, T. Shamspur, A. Mostafavi, Evaluation of GO nanosheets decorated by CuFe₂O₄ and CdS nanoparticles as photocatalyst for the degradation of dinoseb and imidacloprid pesticides, *Ceram. Int.* (2020) 466124–6128.
- [21] M. Motamedi, L. Yerushalmi, F. Haghghat, Z. Chen, Recent developments in photocatalysis of industrial effluents : A review and example of phenolic compounds degradation, *Chemosphere*. 296 (2022) 133688-133697.
- [22] H. Mashhadi kashtiban, H. Rasouli, P.Y. Sefidi, M.G. Hosseini, Polyaniline film decorated with cadmium sulfide- NrGO nanosheet heterostructure hybrid as highly efficient photoelectrocatalyst for water splitting, *Mater. Sci. Semicond. Process.* 141 (2022) 106425-106436.
- [23] J. Xu, H. Olvera-Vargas, F.Y.H. Teo, O. Lefebvre, A comparison of visible-light photocatalysts for solar photoelectrocatalysis coupled to solar photoelectro-Fenton: Application to the degradation of the pesticide simazine, *Chemosphere*. 76 (2021) 130138-130149.
- [24] J.H. Chang, M. Kumar, S.Y. Shen, Agricultural application of visible light photocatalyst, Nanostructured Mater. *Vis. Light Photocatal.* (2021) 467–489.
- [25] H. Sheikhpour, A. Saljooqi, T. Shamspur, A. Mostafavi, Co-Al Layered double hydroxides decorated with CoFe₂O₄ nanoparticles and g-C₃N₄ nanosheets for efficient photocatalytic pesticide degradation, *Environ. Technol. Innov.* 23 (2021) 101649-101658.
- [26] A. Marta, C. Cristina, G. Carlos, L.M. Pastrana-mart, L.F. Adri, S. Marisol, F. Ana, J.L. Faria, A.M.T. Silva, M. Faraldos, A. Bahamonde, B. Tio, BARE TiO₂ AND GRAPHENE OXIDE TiO₂ PHOTOCATALYSTS ON THE DEGRADATION OF THE WATER MATRIX, *Appl. Surf. Sci.* 416 (2015) 1013–1021.
- [27] A. Shahnazi, M.R. Nabid, R. Sedghi, B. Heidari, A thermosensitive molecularly imprinted poly-NIPAM coated MWCNTs/TiO₂ photocatalyst for the preferential removal of pendimethalin pesticide from wastewater, *J. Photochem. Photobiol. A Chem.* 402 (2020) 112802-112815.
- [28] A. Ibrahim, W. Mekprasart, W. Pecharapa, Anatase/Rutile TiO₂ composite prepared via sonochemical process and their photocatalytic activity, *Mater. Today Proc.* 4 (2017) 6159–6165.
- [29] C.B. Anucha, I. Altin, E. Bacaksiz, V.N. Stathopoulos, (2022) Titanium dioxide (TiO₂)-based photocatalyst materials activity enhancement for contaminants of emerging concern (CECs) degradation: In the light of modification strategies, *Chem. Eng. J. Adv.* 10 (2022) 100262-100275.
- [30] M. Zahedifar, N. Seyedi, Bare 3D-TiO₂/magnetic biochar dots (3D-TiO₂/BCDs MNPs): Highly efficient recyclable photocatalyst for diazinon degradation under sunlight irradiation, *Phys. E Low-Dimensional Syst. Nanostructures*. 139 (2022) 115151-115162.
- [31] P. Garcia-Muñoz, F. Fresno, J. Ivanez, D. Robert, N. Keller, Activity enhancement pathways in LaFeO₃@TiO₂ heterojunction photocatalysts for visible and solar light driven degradation of myclobutanil pesticide in water, *J. Hazard. Mater.* 400 (2020) 123099-123111.
- [32] A.N. Fahri, S. Ilyas, M.A. Anugrah, H. Heryanto, M. Azlan, A.T.T. Ola, R. Rahmat, N. Yudasari, D. Tahir, Bifunctional Purposes of Composite TiO₂/CuO/Carbon Dots (CDs): Faster Photodegradation Pesticide Wastewater and High Performance

- Electromagnetic Wave Absorber, *Materialia*. 26 (2022) 101588-101605.
- [33] A. Saljooqi, T. Shamspur, A. Mostafavi, Synthesis of titanium nanoplate decorated by Pd and Fe₃O₄ nanoparticles immobilized on graphene oxide as a novel photocatalyst for degradation of parathion pesticide, *Polyhedron*. 179 (2020) 114371-114380.
- [34] Z. Fu, S. Zhang, Z. Fu, Preparation of multicycle GO/TiO₂ composite photocatalyst and study on degradation of methylene blue synthetic wastewater, *Appl. Sci.* 9 (2019) 9163282-9133290.
- [35] M.R. Gaeeni, M. Tohidian, M. Sasani Ghamsari, M.H. Majles Ara, Synthesis of graphene oxide-TiO₂ nanocomposite as an adsorbent for the enrichment and determination of rutin, *Nanomedicine J.* 2 (2015) 269–272.
- [36]M. Sharma, K. Behl, S. Nigam, M. Joshi, TiO₂-GO nanocomposite for photocatalysis and environmental applications: A green synthesis approach, *Vacuum*.156 (2018) 434–439.
- [37] N. Lv, Y. Li, Z. Huang, T. Li, S. Ye, D.D. Dionysiou, X. Song, Synthesis of GO/TiO₂/Bi₂WO₆ nanocomposites with enhanced visible light photocatalytic degradation of ethylene, *Appl. Catal. B Environ.* 246 (2019) 303–311.
- [38]. Habibi Jetani, M.B. Rahmani, TiO₂/GO nanocomposites: synthesis, characterization, and DSSC application, *Eur. Phys. J. Plus.* 135 (2020) 2173-2182.
- [39]P.M. Martins, C.G. Ferreira, A.R. Silva, B. Magalhães, M.M. Alves, L. Pereira, P.A.A.P. Marques, M. Melle-Franco, S. Lanceros-Méndez, TiO₂/graphene and TiO₂/graphene oxide nanocomposites for photocatalytic applications: A computer modeling and experimental study, *Compos. Part B Eng.* 145 (2018) 39–46.
- [40]S.A. Khan, Z. Arshad, S. Shahid, I. Arshad, K. Rizwan, M. Sher, U. Fatima, Synthesis of TiO₂/Graphene oxide nanocomposites for their enhanced photocatalytic activity against methylene blue dye and ciprofloxacin, *Compos. Part B Eng.*, 175 (2019), 107120-107129.
- [41] H. Zhang, X. Wang, N. Li, J. Xia, Q. Meng, J. Ding, J. Lu, Synthesis and characterization of TiO₂/graphene oxide nanocomposites for photoreduction of heavy metal ions in reverse osmosis concentrate, *RSC Adv.* 8 (2018) 34241–34251.
- [42]R. Razavi, M. Basij, H. Beitollahi, S. Panahandeh, Experimental and theoretical investigation of acetamiprid adsorption on nano carbons and novel PVC membrane electrode for acetamiprid measurement, *Sci. Rep.* 12 (2022) 16459-16465.
- [43] R. Razavi, S.M.A. Hosseini, M. Ranjbar, Production of nanosized synthetic rutile from ilmenite concentrate by sonochemical HCl and H₂SO₄ leaching, *Iran. J. Chem. Chem. Eng.* 33 (2014) 29–36.
- [44]I.M. Joni, L. Nulhakim, C. Panatarani, Characteristics of TiO₂ particles prepared by simple solution method using TiCl₃ precursor, *J. Phys. Conf. Ser.* 1080 (2018) 012042-012049.
- [45] A. Haider, Z. Jameel, S. Taha, Synthesis and Characterization of TiO₂ Nanoparticles via Sol-Gel Method by Pulse Laser Ablation, *Eng. Technol. J.* 33 (2015) 761–771.



COPYRIGHTS

© 2022 by the authors. Licensee PNU, Tehran, Iran. This article is an open access article distributed under the terms and conditions of the Creative Commons Attribution 4.0 International (CC BY4.0) (<http://creativecommons.org/licenses/by/4.0>)

حذف آمیتراز توسط نانو میله های دی اکسید تیتانیوم

راضیه رضوی^{۱*}، مسلم بسیج^۲، مرضیه سلاجقه^۱

گروه شیمی، دانشکده علوم، دانشگاه جیرفت، جیرفت، ایران

گروه گیاهپزشکی، دانشکده کشاورزی، دانشگاه جیرفت، جیرفت، ایران

* E-mail: r.razavi@ujiroft.ac.ir

تاریخ پذیرش: ۱۴ شهریور ۱۴۰۳

تاریخ دریافت: ۱۸ خرداد ۱۴۰۳

چکیده

حذف آمیتراز توسط TiO_2 سنتز شده از محلول آبی مورد بررسی قرار گرفت. برای این پیشنهاد، FT-IR، XRD، UV-Vis، SEM و EDS برای توصیف نانوجاذب‌های سنتز شده و تعیین فرآیند حذف استفاده شد. مطالعات جذب دسته ای برای بررسی اثر دما، غلظت اولیه آمیتراز، تعداد جاذب و زمان تماس به عنوان پارامترهای مهم جذب انجام شد. حداکثر زمان تعادل ۱۵ دقیقه با ۵ میلی گرم جاذب در دمای ۳۵ درجه سانتیگراد در pH=7 برای TiO_2 بود. همه داده‌های تعادل جذب به خوبی با مدل ایزوترم فروندلیخ با رفتار ناهمگن، چند لایه، وابسته به دما، برگشت‌ناپذیر و خودبه‌خود مطابقت داشتند.

کلید واژه ها

آمیتراز؛ حذف؛ TiO_2 ؛ جاذب ایزوترم؛ سینتیک.